Bioinformatics, Proteomics and Immaging Analysis

OMMEGA Publishers
Answering Intelligence
www.ommegaonline.org

Research Article

OPEN ACCESS

Sequence to Structure Analysis of SOD1 and SOD2 from Fresh Water Turtles

Rituparna Sarma[1#], Dhirendra K Sharma[2*]

[1]Bioinformatics Centre, Gauhati University, Guwahati, Assam, India
[2]School of Biological Sciences, University of Science and Technology, Meghalaya, Techno city, Baridua, India
[*]RS and DKS designed the research work. Manuscript was prepared and verified by both the authors.
[#]RS carried out the experiments.

Corresponding Author: Dhirendra Kumar Sharma, School of Biological Sciences, University of Science and Technology, Meghalaya, Techno city, Kiling Road, Baridua-793101, India. Tel: +91 9435147412; E-mail: dksgu@yahoo.co.uk

Abstract

Superoxide dismutase (SOD) responsible for dismutation of ROS produced in cell controls the aging and longevity of animals. An attempt has been made to report on sequence to structure analysis of the genes and proteins of SOD1 and SOD2 of freshwater turtles, *Pelodiscus sinensis* and *Mauremys reevesii*. Analysis of gene and protein sequences of these SODs retrieved from the NCBI database suggested that the there were minor variations in their molecular weight of the gene sequences, melting temperature, folding, aliphatic index and isoelectric point. Gene sequences were all AT rich with 5 restriction sites each in SOD1 of both the turtles and SOD2 of *Pelodiscus sinensis* while 8 restriction sites in SOD2 of *Mauremys reevesii* were obtained. SOD1 were dominated by β Strands, whereas, SOD2 were by the alpha helices. Homology models were generated by MODELLER 9.12 presented that all the models of SODs within acceptable range. Solvent accessible surface area (SASA) and active sites analysis of refined models of the SOD proteins were acidic and with 5 to 11 number of active sites in all the proteins and high percentage of exposed aliphatic residues. Therefore, it could well be inferred that these models have the potentiality to be used for understanding the aging process.

Keywords: SOD1; SOD2; Structural characterization of Protein; Turtles *P. sinensis; M. reevesii*

Received Date: June 17, 2015
Accepted Date: September 28, 2015
Published Date: October 06, 2015

Citation: Sarma, R. and Sharma, D.K., Sequence to Structure Analysis of SOD1 and SOD2 from Fresh Water Turtles. (2015) Bioinfo Proteom Img Anal 1(2): 38- 43.

DOI: 10.15436/2381-0793.15.006

Introduction

Superoxide dismutase (SOD) is the most effective enzyme in the aging process and longevity, regulates the Reactive Oxygen Species (ROS), produced in the metabolic and physiological events of animals[1-3]. Unbalanced concentration of ROS often contributes to diseases like cancer, diabetes, premature aging, inflammation and hypertension[4]. The SOD1 is found in cytoplasm and outer mitochondrial space, protects the cells against any lethal effects of radiation, drugs or toxicity of ROS[5]while the SOD2 found in inner mitochondrial space, promotes cellular differentiation, apoptosis, tumorgenesis and hypoxia induced pulmonary disease[6-9]. Among all the Superoxide dismutase found in organisms, only the SOD1 (Cu, Zn SOD) and SOD2 (Mn SOD) have been sequenced so far in a limited number of chelonians, but without structural information[10]. The group turtles, many of them survived for a prolonged period and that too with very active life has been an interesting model to understand the aging[11,12]. Reliable 3-D structural predictions using Homology modeling of these proteins might be significant to understand the aging process[13]. *Pelodiscus sinensis* Wiegmann, 1835 and *Mauremys reevesii* Grey, 1831 are the two freshwater turtles[14] have often been used as models for turtle evolution and development studies, where SOD1 and SOD2 have been sequenced recently[15-17]. Therefore, an attempt has been made to analyze the SOD gene and protein sequences and their characterization (SOD1 and SOD2) in *Pelodiscus sinensis* and *Mauremys reevesii* at structural and functional level. Prediction of the secondary structures, analysis of gene and protein sequence properties, restriction sites, homology modeling and evaluation, Solvent Accessible Surface Area (SASA) and

active site prediction of the SODs of *Pelodiscus sinensis* and *Mauremys reevesii* were carried out to understand their structural and functional status.

Methods

Sequence Retrieval and Sequence Analysis

SOD nucleotide and protein sequences of *Pelodiscus sinensis* (**GenBank SOD1: GenBank: JX470524.1, GenPept: AEK80392.1, SOD2: GenBank: JX470525.1, GenPept: AEK22120.1**) and *Mauremys reevesii* (**SOD1: GenBank: JX843790.1, GenPept: AFX95918.1, SOD2: GenBank: JX843791.1, GenPept: AFX95919.1**) were retrieved from NCBI. Sequence lengths of SOD1 (155 aa) and SOD2 (226 aa) were similar in both the turtle species. Nucleotide lengths of SOD1 were 727 bp and 749 bp, while the SOD2 had 1436 bp and 1687 bp in *Pelodiscus sinensis* and *Mauremys reevesii* respectively. Nucleotide and protein sequences were run in **CLC workbench package (CLC Bio)**[18] to analyze sequence properties, secondary structure prediction as well the restriction sites. Clustal W2 program[19] was used to align the protein sequences.

Homology Modeling of Protein and Evaluation

The 3D structures of SOD1 and SODs were generated using comparative method in MODELLER 9.12[20]. Validation of the models was done by PROCHECK[21] and RAMPAGE[22]. The minimization of energy and refinement of protein structures were carried out by Discovery Studio package (Accelrys)[23] and Chiron[24]. Refined structures were evaluated using PROSESS[25], PROCHECK and RAMPAGE and ProFunc[26].

Solvent Accessible Surface Area (SASA) and Active Site Prediction

SASA and active site predictions were carried out by using the best refined model structures of the proteins. Get Area[27], Discovery Studio Client 4.0 was used to find out the SASA percentage. Active sites and cleft predictions of SOD1 and SOD2 were determined by Active Site Prediction and Analysis Server, DoG Site Scorer[28] and ProFunc. DoG Site Scorer identifies all cavities in a protein and analyses the amino acid composition of each cavities. It scores the cavities by functional protein lining around them based on their physicochemical properties. Amino acid residue types were evaluated at the largest pocket and clefts.

Results

Nucleotide Sequence Analysis

Sequence Retrieval and Sequence Analysis:

SOD1 and SOD2 nucleotide sequences of *Pelodiscus sinensis* and *Mauremys reevesii* were downloaded from the NCBI database. Molecular weight for SOD1 was 236.155kDa and 243.483 kDa, whereas for SOD2 it was 463.464kDa and 544.515kDa in *Pelodiscus sinensis* and *Mauremys reevesii* respectively. The genes were found to be AT rich. (Table 1)

Table 1: Comparative Nucleotide sequence statistics of the SODs of *Pelodiscus sinensis* and *Mauremys reevesii*

Information	SOD1		SOD2	
	P. sinensis	*M. reevesii*	*P. sinensis*	*M. reevesii*
Length (bp)	727	749	1436	1687
Molecular Weight (kDa)	236.155	243.483	463.464	544.515
Melting Temperature [Salt]=0.1M Ĉ	82.78	81.76	81.35	82.11
C+G count	317	308	576	708
A+T count	410	441	860	979

Restriction Enzyme Digestion

The nucleotide SOD sequences were restriction digested *in- silico* with 8 restriction enzymes namely, BglII, EcoRI, FokI, HindIII, MspI, PstI, SmaI and XbaI based on 4-base and 6-base cutters, virtual gene map of the gene sequences (Table 2). Results showed that the Gene sequences of SOD1 and SOD2 of *Pelodiscus sinensis* have 5 restriction sites, while the SOD2 of *Mauremys reevesii* presented 8 restriction sites.

Table 2: Various restriction cuts and position of the SOD gene against 8 different restriction enzyme in *Pelodiscus sinensis* and *Mauremys reevesii*

Name of Restriction enzymes	Pattern	Over-hang	SOD1 of *Pelodiscus sinensis (cut positions)*	SOD1 of *Mauremys reevesii (cut positions)*	SOD2 of *Pelodiscus sinensis (cut positions)*	SOD2 of *Mauremys reevesii (cut positions)*
BglII	agatct	5'	280,492 (2)	281,493 (2)	-	-
EcoRI	gaattc	5'	-	-	-	930
FokI	ggatg	5'	213	214, 273 (2)	-	171,555 (2)
HindIII	aagctt	5'	-	602	898, 1189 (2)	963, 1442 (2)
MspI	ccgg	5'	116	-	57	24
PstI	ctgcag	3'	63	-	521	585
SmaI	cccggg	Blunt	-	-	-	25
XbaI	tctaga	5'	-	-	106	-
Total Number of cuts			5	5	5	8

Protein Sequence Analysis

Analysis of protein sequences for SOD1 of *Pelodiscus sinensis* had molecular weight 15.819 kDa, isoelectric point 6.47 with aliphatic index at 76.71 whereas SOD1 of *Mauremys reevesii* had 16.022 kDa molecular weight, isoelectric point 6.87 and aliphatic index at 82.97.SOD2 in *Pelodiscus sinensis* demonstrated molecular weight of 25.166 kDa, isoelectric point 9.01 and aliphatic index 83.319 compared to 25.049 kDa, 9.04 and 83.761 respectively for SOD2 of *Mauremys reevesii* (Table 3).

Table 3: Comparison of residue types of SOD1 and SOD2 between *Pelodiscus sinensis* and *Mauremys reevesii*

Residue types	SOD1 (*Pelodiscus sinensis*)		SOD1 (*Mauremys reevesii*)		SOD2 (*Pelodiscus sinensis*)		SOD2 (*Mauremys reevesii*)	
Hydrophobicity	Count	Frequency	Count	Frequency	Count	Frequency	Count	Frequency
Hydrophobic (A,F,G,I,L,M,P,V,W)	80	0.516	80	0.516	115	0.509	112	0.496
Hydrophilic (C,N,Q,S,T,Y)	36	0.232	34	0.219	62	0.274	65	0.288
Others	39	0.252	41	0.265	49	0.217	49	0.217
Charge type	**Count**	**Frequency**	**Count**	**Frequency**	**Count**	**Frequency**	**Count**	**Frequency**
Negatively Charged (D & E)	19	0.123	17	0.110	18	0.080	18	0.080
Positively Charged (R & K)	15	0.097	14	0.090	22	0.097	22	0.097
Other	121	0.781	124	0.800	186	0.823	186	0.823
Dominant residue								
Glycine (SOD1)	27	0.174	25	0.161	-	-	-	-
Luecine (SOD2)	-	-	-	-	25	0.111	25	0.111

Model Prediction and Evaluation

MODELLER 9.12 was used to predict the 3D structures of SOD1s and SOD2s for *P. sinensis* and *M. reevesii*. Final templates selected for MODELLER 9.12 were as follows; for SOD1, 3GTV_A (153aa, 78% identical for *P. sinensis*) and 3GTT_A (153aa and 75% identical for *M. reevesii*) and for SOD2, 1PL4_A (198aa, 89% identical for *P. sinensis*) and 1NOJ_A (199 aa, 86% identical for *M. reevesii*). In MODELLER, 3D structures were generated comparing target sequences with the help of template sequences and aligned with the maximum similar structure on the basis of DOPE Score and mole PDF Score. In PROCHECK analysis, SOD1 of *P. sinensis* and *M. reevesii* scored 91.0% and 89.5% while the SOD2 scored at 92.7% and 96.7% respectively. On the other hand, in RAMPAGE analysis, SOD1 secured 98.0% against 98.7% in SOD2 for *P. sinensis* while SOD1 and SOD2 of *M. reevesii* scored 97.4% and 98.6% respectively. The SOD1 and SOD2 models were refined using Chiron by minimizing the number of clashes (non-physical atomic interactions, Figure1. Refined SOD1 of *P. sinensis* and *M. reevesii* scored 81.1% and 89.5%, while the refined SOD2s scored 91.6% and 96.7% respectively for both the turtle groups in PROCHECK analysis. In RAMPAGE analysis SOD1 models scored 94.1% and 94.8% against SOD2 which scored 96.0% and 98.0% for *P. sinensis* and *M. reevesii* respectively. G-Factor scores of all the structures were found to be usual. Refinement analysis suggested that the structure for SOD1 and SOD2 of *M. reevesii* were more stable than *P. sinensis*. Refined models were used for further analysis.

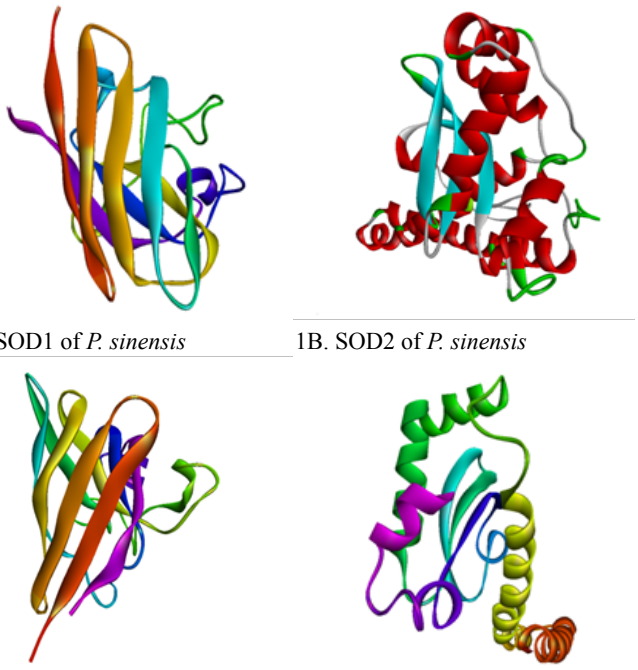

1A. SOD1 of *P. sinensis* 1B. SOD2 of *P. sinensis*

1C. SOD1 of *M. reevesii* 1D. SOD2 of *M. reevesii*

Figure 1: Refined structures of SOD 1 and SOD 2 of *P. sinensis* and *M. reveesii*

PROSESS analysis showed that SOD1s of the turtle(s) had 47% β-Strands, while 17% was present in SOD2 of *M. reevesii*, compared to 12% of SOD2 in *P. sinensis*. β-strand and coil dominated the SOD1 structures with only 2-3% helix in both the models. In SOD2, helix was noted to be dominating the model with 58% in *M. reevesii* against the 50% in the model of *P. sinensis*. Covalent bond and packaging bond qualities were within the acceptable range for all the SOD structures.

Discovery studio 4.0 calculated that the refined SOD1 of *P. sinensis* had 1366nos. of atom at a molecular weight of 15,801.8 kDa with net formal charge (-2) demonstrating the chemical formula as $C_{675}\ H_{1088}\ N_{206}\ O_{222}\ S_5$, while the SOD2 had 2,177 number of atoms, molecular weight of 25,139.8kDa and net formal charge of 5 presenting the chemical formula $C_{1129}H_{1747}\ N_{316}\ O_{320}\ S_9$. Whereas, SOD1 of *M. reevesii* had 1,383 atoms, 16,003.1 kDa molecular weight, net formal charge -3 showing the chemical formula as $C_{685}\ H_{1109}\ N_{208}\ O_{224}\ S_5$ and the SOD2 had 1,417 atoms, 16,434.7 kDa molecular weight, net formal charge (-1) with chemical formula $C_{747}\ H_{1126}\ N_{197}\ O_{217}\ S_3$. The net formal charge indicated that the SOD1 of *P. sinensis* as well the SOD1 of SOD2 of *M. reevesii* had higher anion atoms, whereas, the SOD2 of *P. sinensis*, (MODELLER) had large numbers cationic charge. All the SODs were of single stranded. The size of the exposed protein groups were found to be higher than the size of the buried protein groups in all the SODs. Hydrophilic residue size was higher than the hydrophobic residue size in SOD1s, while vice-versa was detected in SOD2s.

Solvent Accessible Surface Area (SASA) and Active site predictions

Get Area server analysis predicted that the total solvent accessibility of SOD1s were 7508.24 and 7835.29 as well for SOD2 was 13424.35 and 8767.77 respectively for *P.sinensis* and *M. reevesii*. A polar surface area was found to be dominant in all the proteins. Likewise, in Discovery studio it was found that solvent accessibility for SOD1 and SOD2 was 7,663.26 and

13,724.3 for *P. sinensis* models while 7,978.09 and 8,964.37 was achieved for *M. reevesii* respectively.

The pocket properties were tabulated in (Table 4). The largest active site volume (Å^3) in SOD1 of *P. sinensis* was 579.50 against 333.06 in *M. reevesii*, whereas, the SOD2 had presented the largest active site volume with 559.17 and 991.94 respectively for both the model of *P. sinensis* and *M. reevesii*. Gly residue was found to be dominant in both the largest active sites of SOD1 models followed by Val residues. Hydrophobicity ratio of 0.38 of SOD1 model in *M. reevesii* was better than the 0.52 of *P. sinensis* in the largest active site. However, in SOD2 model, the largest pockets had the highest number of amino acid residues of Gly and Leu in both the *P. sinensis* and *M. reevesii* models with hydrophobicity ratio of 0.49 and 0.65 respectively. ProFunc results showed that the SOD1 models of *P. sinensis* and *M. reevesii* had the largest cleft size of 2045.67 Å and 2234.67 Å, while SOD2 had 1666.41 Å and 2122.88 Å respectively. Comparison of residue types in the largest clefts suggested that the SOD1 model of *P. sinensis* had dominant equal numbers of positive, neutral and aliphatic residues (10 residues in each) while the model of *M. reevesii* was aliphatic residue dominant (11 residues in each) followed by negative residues (10 residues). The SOD2 was with positive and neutral residues (6 residues each) however, was dominant in the model of *P. sinensis* while aliphatic (11 residues) followed by aromatic residues (10 residues) were dominant in the model of *M. reevesii*.

Table 4: Cavity size and properties of SOD1 and SOD2 of *P. sinensis* and *M. reevesii* analyzed using DogSiteScorer server

P. sinensis						*M. reevesii*					
SOD1			SOD2			SOD1			SOD2		
Name	Volume [Å^3]	Surface [Å^2]	Name	Volume [Å^3]	Surface [Å^2]	Name	Volume [Å^3]	Surface [Å^2]	Name	Volume [Å^3]	Surface [Å^2]
P0	597.50	1253.23	P0	559.17	997.41	P0	333.06	676.03	P0	991.94	1277.61
P1	180.22	426.61	P1	351.55	492.69	P1	228.67	506.07	P1	234.30	519.95
P2	176.13	352.34	P2	281.15	582.44	P2	220.67	483.83	P2	186.50	421.61
P3	166.08	271.72	P3	172.74	352.86	P3	178.94	414.18	P3	123.20	252.73
P4	156.93	390.76	P4	170.62	463.47	P4	127.49	406.82	P4	104.96	277.51
P5	104.64	447.23	P5	162.69	294.43	P5	120.70	143.76			
			P6	137.92	367.72	P6	111.68	346.16			
			P7	118.78	224.80						
			P8	115.58	257.74						
			P9	107.71	191.29						
			P10	101.25	382.66						

Discussion

Nucleotide base composition analysis of SOD1s and SOD2s suggested that all the genes were AT rich where 'Adenine' was dominating (Table 1). DNA replication starts at the AT rich regions and these regions are universally the most conserved regions found in replicons[29-31]. In both the SOD1, adenine percentage was followed by almost the same frequency ranges for guanine, thymine and low percentage for cytosine. While in SOD2, adenine percentage is marginally higher than the thymine followed by guanine and low cytosine percentage. Analysis of SOD1 and SOD2 nucleotide sequences showed that that there were minor variations in melting temperatures and no coding regions were defined in the sequences. *In silico* analysis of restriction site variability has been suggestive of their differences may lead to high degree of polymorphism. Further, similarity in the conserved sequence is in fact suggestive predicted their identical longevity.

Aliphatic index of SOD1 of *Mauremys reevesii* were higher, indicative of its stability over different temperatures ranges than the SOD1 of *Pelodiscus sinensis*. Isoelectric point indicated that the pH of both the SOD1 were acidic when not carrying any net electrical charge. Results indicated that SOD2 of *Mauremys reevesii* had more stability than the SOD2 of *Pelodiscus sinensis*. Half-life of all the SODs were > 20 hrs. SOD1 of both the turtles had the similar frequency of hydrophobic residues, but there were variations in frequencies of hydrophilic residue with both the negative and positive charges. Where as in case of SOD2, charged residue frequencies were of same but there were variations in frequencies of hydrophobic and hydrophilic residues. Glycine (G) residue distribution was found to be dominant in both the SOD1, while the distribution frequency of leucine (L) was dominant in SOD2s. Due to dominance of Glycine, helix forming probabilities were low in SOD1, while such helix forming probabilities were evident in the SOD2 with leucine dominance. Moreover, all the four SOD sequences might be highly conserved since the Glycine and Leucine have low mutability and are more frequent in conserved sequence elements[32].

Prediction of secondary structures locates the positions of the amino acid residues, whether they lie in helixes, strands or in coils[33]. Secondary structure prediction indicated that the SOD1 of both the *Pelodiscus sinensis* and *Mauremys reevesii* had same 12 numbers of β strands with no α helices. Though the number of beta strands was same, yet variations at the 2nd, 3rd and 4th strand positions of both the structures were noticed. SOD2 of *Pelodiscus sinensis* had 13 α helices and 4 β strands compared to 12 α helices and 5 β strands of SOD2 from *Mauremys reevesii*. The structure was suggestive of the dominance of α helix in both the SOD2. Further, sequence alignment suggested that the SOD1 and SOD2 of both the turtles had 90.32% and 97.78% conserved sequence similarity respectively.

From the ProFunc evaluation, it could be outlined that all the proteins were associated with cellular oxygen and reactive oxygen species and metabolic processes. SASA prediction helps in understanding the probable binding oriented conformational changes that may occur in the protein structures[34]. It could be suggested from the results that the models had greater potentiality of binding to the ligands in solvent.

Active site predictions are essential for prediction of functions, classification and drug binding ability of proteins[35]. It has been found that SOD1 of *P. sinensis* had 6 numbers of pockets against the model of *M. reevesii*, which had 7 pockets; on the other hand, the SOD2 had 11 and 5 numbers of pockets for the models of *P. sinensis* and *M. reevesii* respectively.

The aromatic residues at the active sites stabilize the monomers in a hydrophobic core. Since the binding site affinities and specificities are mainly achieved by hydrogen bond interactions[36], the results of active sites and clefts predictions, it could well be inferred that both the SOD1 and SOD2 proteins of the two turtles had acceptable and applicable range of active sites and cavity size.

Conclusion

Analysis of the nucleotide sequences of the SODs suggested that the genes were AT rich and had minor melting temperature differences with good number of restriction sites indicate high degree of polymorphism. Analysis of protein sequences of SOD1 and SOD2 and evaluation of the predicted secondary and tertiary refined structures of the two SODs generated by MODELLER 9.12 indicated that all the 4 SODs structure (s) were within acceptable range. Comparison among the models with their counterparts suggested that although they had the sequence similarity of around 90%, yet all the SODs had their own individual structural characteristics. SOD structures were submitted to PMDB database under the IDs PMDB ID: PM0079765 (SOD1 of *P. sinensis*), PMDB ID: PM0079766 (SOD2 of *P. sinensis*), PM0079772 (SOD1 of *M. reevesii*) and PM0079773for SOD2 of *M. reevesii*. Thus it could be assumed that these models and the data have the potentiality to be used as source for further understanding on the aging process and drug binding related attempts.

Conflict of Interest: There was no conflict of interest.

Acknowledgement

All the researches were carried out in Bioinformatics Facility Centre (BIFGU), Gauhati University as well in the Department of Zoology of the University of Science and Technology, Meghalaya. The authors gratefully acknowledge Department of Biotechnology (DBT), Government of India for their help and assistance.

References

1. Fridovich, I. Superoxide dismutase. An adaptation to a paramagnetic gas. (1989) J Biol Chem 264(14): 7761 -7764.
2. Harman, D. Aging: A theory based on free radical and radiation chemistry. (1956) J Gerontol 11(3): 298–300.
3. Harman, D. Aging: Prospects for further increases in functional life span. (1994) Age 17(4): 119–146.
4. Zelko, I.N., Mariani, T.J., Folz R.J. Superoxide dismutase multigene family: a comparison of the CuZn-SOD (SOD1), Mn-SOD (SOD2), and EC-SOD (SOD3) gene structures, evolution, and expression. (2002) Free Radic Biol Med 33(3): 337-349.
5. Epstein, C.J., Avraham, K.B., Lovett, M., et al. Transgenic mice with increased Cu/Zn-superoxide dismutase activity: animal model of dosage effects in Down syndrome. (1987) Proc Natl Acad Sci 84(22): 8044-8048.
6. Scott, M.D., Meshnick, S.R., Eaton J.W. Superoxide dismutase amplifies organismal sensitivity to ionizing radiation. (1989) J Biol Chem 264(5): 2498–2501.
7. Wispe, J.R., Warner, B.B., Clark, J.C., et al. Human Mn-superoxide dismutase in pulmonary epithelial cells of transgenic mice confers protection from oxygen injury. (1992) J Biol Chem 267(33): 23937–23941.
8. St. Clair, D.K., Oberley, T.D., Muse, K.E., et al. Expression of manganese superoxide dismutase promotes cellular differentiation. (1994) Free Radic Biol Med 16(2): 275–282.
9. Landis, G.N., Tower, J. Superoxide dismutase evolution and life span regulation. (2005) Mech Ageing Dev 126(3): 365-379.
10. Willmore, W.G., Storey, K.B. Antioxidant systems and anoxia tolerance in a freshwater turtle Trachemys scripta elegans. (1997) Mol cell Biochem 170(1-2): 177-185.
11. Warner, H.R. Superoxide dismutase, aging, and degenerative disease. (1994) Free Radic Biol Med 17(3): 249-258.
12. Krivoruchko, A., Storey, K.B. Forever young: Mechanisms of natural anoxia tolerance and potential links to longevity. (2010) Oxid Med Cell Longev 3(3): 186-198.
13. Sarma, R., Verma, A., Sharma, D.K. et al. 3D structure prediction of aging related proteins of Silurana tropicalis Gray 1864. (2013) J Pharmacy Res 7(8): 762-765.
14. Rhodin, A.G.J., Dijk, P.P.V., Iverson, J.B., et al. Turtles of the World Update: Annotated Checklist of Taxonomy, Synonomy, Distribution and Conservation Status. (2010) Chelonian Res Monographs 5: 85–164.
15. Wang, Z., Pascual-Anaya, J., Zadissa, A., et al. The draft genomes of soft-shell turtle and green sea turtle yield insights into the development and evolution of the turtle-specific body plan. (2013) Nat Genet 45(6): 701-706.
16. Peng, Q., Pu You, G., Wang Zhi, F., et al. Complete mitochondrial genome sequence analysis of Chinese softshell turtle (Pelodiscussinensis). (2005) Chinese J Biochem Mole Biol 21(5): 591-596.
17. Parham, J.F., Macey, J.R., Papenfuss, T.J., et al. The phylogeny of Mediterranean tortoises and their close relatives based on complete mitochondrial genome sequences from museum specimens. (2006) Mol Phylogenet Evol 38(1): 50-64.
18. Chang, G.H., Lin, L., Luo, Y.J., et al. Sequence analysis of six enterovirus 71 strains with different virulences in humans. (2010) Virus Res 151(1): 66-73.
19. Edgar, R.C. MUSCLE: Multiple sequence alignment with high accuracy and high throughput. (2004) Nucleic Acids Res 32(5): 1792-1797.
20. Verma, A., Sharma, D.K., Sarma, R., et al. Comparative insights using the molecular homology model of BDNF (Brain derived neurotrophic factor) of Varanuskomodoensis and the known NGF (Nerve growth factor) structure of Najaatra. (2013) Bioinformation 9(15): 755-758.
21. Laskowski, R.A., MacArthur, M.W., Moss, D.S., et al. PROCHECK: A program to check the Stereochemical quality of protein structures. (1993) J Appl Cryst 26: 283-291.
22. Lovell, S.C., Davis, I.W., Arendall, W.B., et al. 2003. Structure validation by Calpha geometry: phi, psi and Cbeta deviation. Proteins 50(3): 437-450.
23. Zhang, Y.R., Zhao, Y.Q., Huang, J.F. Retinoid-binding proteins: similar protein architectures bind similar ligands via completely different ways. (2012) PLoS One 7(5): e36772.
24. Ramachandran, S., Kota, P., Ding, F., et al. Automated minimization of steric clashes in protein structures. (2011) Proteins 79(1): 261-270.
25. Berjanskii, M. PROSESS: A protein structure evaluation suite and server. (2010) Nucleic acids Res 38: W633-W640.
26. Laskowski, R.A., Watson, J.D., Thornton, J.M. ProFunc: A server for predicting protein function from 3D structure. (2005) Nucleic Acids Res 33: W89-W93.
27. Fraczkiewicz, R., Braun, W. Exact and efficient analytical calculation of the accessible surface areas and their gradients for macromolecules. (1998) J Comput Chem 19(3): 319-333.
28. Volkamer, A., Kuhn, D., Grombacher, T., et al. Combining global and local measures for structure-based druggability predictions. (2012) J Chem Inf Model 52(2): 360-372.
29. Bell, S.P., Dutta, A. DNA replication in eukaryotic cells. (2002) Annu Rev Biochem 71: 333–374.
30. Konieczny, I. Strategies for helicase recruitment and loading in bacteria. (2003) EMBO Rep 4(1): 37–41.

31. Rajewska, M., Weqrzyn, K., Koniecznyl, I. AT-rich region and repeated sequences–the essential elements of replication origins of bacterial replicons. (2012) FEMS Microbiol Rev 36(2): 408-434.
32. Brooks, D.J., Fresco, J.R. Increased frequency of cysteine, tyrosine, and phenylalanine residues since the last universal ancestor. (2002) Mol Cell Proteomics 1(2): 125-131.
33. Kumar, N.V., Rani, M.E., Gunaseeli, R., et al. Modeling and structural analysis of cellulases using Clostridium thermocellum as template. (2012) Bioinformation 8(22): 1105-1110.
34. Marsh, J.A., Teichmann, S.A. Relative solvent accessible surface area predicts protein conformational changes upon binding. (2011) Structure 19(6): 859-867.
35. Gao, M., Skolnick, J. A comprehensive survey of small-molecule binding pockets in proteins. (2013) PLoS comput Biol 9(10): e1003302.
36. Quiocho, F.A. Atomic structures of periplasmic binding proteins and the high-affinity active transport systems in bacteria. (1990) Philos Trans R Soc Lond B Biol Sci 326(1236): 341-352.

Ommega Online Publisher
Bioinformatics, Proteomics and Immaging Analysis
Short Title : Bioinfo Proteom Img Anal

ISSN: 2381-0793
E-mail : bioinfo@ommegaonline.org
website: www.ommegaonline.org